

Stable Dynamic Walking over Rough Terrain

Theory and Experiment

Ian R. Manchester, Uwe Mettin, Fumiya Iida, and Russ Tedrake

Abstract We propose a constructive control design for stabilization of non-periodic trajectories of underactuated mechanical systems. An important example of such a system is an underactuated “dynamic walking” biped robot walking over rough terrain. The proposed technique is to compute a transverse linearization about the desired motion: a linear impulsive system which locally represents dynamics about a target trajectory. This system is then exponentially stabilized using a modified receding-horizon control design. The proposed method is experimentally verified using a compass-gait walker: a two-degree-of-freedom biped with hip actuation but pointed stilt-like feet. The technique is, however, very general and can be applied to higher degree-of-freedom robots over arbitrary terrain and other impulsive mechanical systems.

1 Introduction

It has long been a goal of roboticists to build a realistic humanoid robot. Clearly, one of the most fundamental abilities such a robot must have is to walk around its environment in a stable, efficient, and naturalistic manner.

When one examines the current state of the art, it seems that one can have either *stability and versatility* or *efficiency and naturalism*, but not all four. This paper reports some recent efforts to bridge this gap.

I.R Manchester · U. Mettin
Department of Applied Physics and Electronics, Umeå University, SE-901 87 Umeå, Sweden.
Tel.: +46-90-786 58 05
Fax: +46-90-786 64 69
e-mail: Ian.Manchester@tfe.umu.se

F. Iida · R. Tedrake
Computer Science and Artificial Intelligence Lab, Massachusetts Institute of Technology, Cambridge MA, 02139, USA.

We propose a general method of exponentially stabilizing arbitrary motions of underactuated mechanical systems. In particular, we develop a provably-stable feedback control strategy for efficient “dynamic walking” bipeds over uneven terrain, and demonstrate experimentally that the method is feasible and effective.

1.1 Bipedal Walking Robots

The world of bipedal walking robots can be divided into two broad classes. The first, including well-known robots such as the Honda ASIMO and the HRP-2, are based on the “zero moment point” (ZMP) principle (see, e.g., [1] and references therein). The main principle of stability and control is that the center of pressure always remains within the polygon of the stance foot, and so the foot always remains firmly planted on the ground. Satisfaction of this principle ensures that all dynamical degrees of freedom remain fully actuated at all times, and thus control design can be performed systematically using standard tools in robotics. However, the motions which are achievable are highly conservative, inefficient, and unnatural looking.

The second broad class consists of passive-dynamic walkers and limit-cycle walkers. Inspired by the completely passive walkers of McGeer [2], these robots forgo full actuation and allow gravity and the natural dynamics to play a large part in the generation of motion. They may be completely passive, or partially actuated. Even with partial actuation, the motions generated can be life-like and highly efficient energetically [3]. However, there is presently a lack of tools for systematic control design and systems analysis.

Comparatively little work has been done as yet on walking over rough terrain, especially for underactuated dynamic walkers. The problem of footstep planning has been approached using computational optimal control [4] and experimental studies have shown that a minimalistic open-loop control can achieve stability for the compass-gait walker [5]. Recently, more complete planning and control systems have been developed for quadruped walkers: see, e.g., [6].

To give the present paper context, in Fig. 1 we depict a possible organizational structure for the perception and control of a dynamic walker on rough terrain. The main components are:

1. **Terrain Perception:** fusion of sensors such as vision, radar, and laser, perhaps combined with pre-defined maps, generating a model of the terrain ahead.
2. **Motion Planning:** uses the terrain map, current robot state, and a model of the robot’s dynamics to plan a finite-horizon feasible sequence of footstep locations and joint trajectories. Slow time-scale: motion plan might be updated once per footstep.
3. **Motion Control:** feedback control to stabilize the planned motion in the face of inaccurate modelling, disturbances, time delays, etc. Fast time-scale: typically of the order of milliseconds.

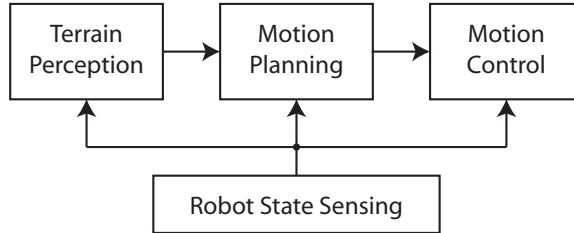


Fig. 1 Possible organization of perception and control of a walking robot.

4. **Robot State Sensing:** optical encoders, accelerometers, gyros, foot pressure sensors, and so on. Provides local information about the physical state of the robot to all other modules.

A complete humanoid robot would have all these components, and many others. In this paper, we focus our attention on component 3: motion control. That is, we assume that the terrain has been sensed and a motion plan generated, and the task remaining is to compute a stabilizing feedback controller which achieves this motion.

1.2 Motion Control for Walking Robots

The problem of motion control of a compass-gait walker has been approached via energy-shaping and passivity-based control techniques (see, e.g., [7, 8, 9]). However, it is not clear how such methods can be extended to robots with more degrees of freedom, or to walking on uneven terrain.

Most tools for underactuated walking make use of Poincaré-map analysis (see, e.g., [10, 11, 12, 13, 14, 15] and many others). For a mechanical system of state dimension $2n$, one constructs a *Poincaré section*: a $(2n - 1)$ -dimensional surface transverse to the orbit under study (e.g. $S(0)$ in Fig. 2). By studying the behaviour of the system only at times at which it passes through this surface, one obtains a $(2n - 1)$ -dimensional discrete time system, the *Poincaré map*:

$$x_{\perp}(k+1) = \mathcal{P}[x_{\perp}(k)], \quad x_{\perp}(\cdot) \in \mathbb{R}^{2n-1}$$

which has a fixed point at the periodic orbit: $\mathcal{P}[x_{\perp}^*] = x_{\perp}^*$. Stability or instability of this reduced system corresponds to orbital stability and orbital instability, respectively, of the periodic orbit. Exponential orbital stability corresponds to all the eigenvalues of the linearization of \mathcal{P} being inside the unit circle.

One disadvantage of the Poincaré map is that it does not give a continuous representation of the dynamics of the system transverse to the target orbit, but focuses only at *one* point on the orbit. This means it has limited use for constructive control design.

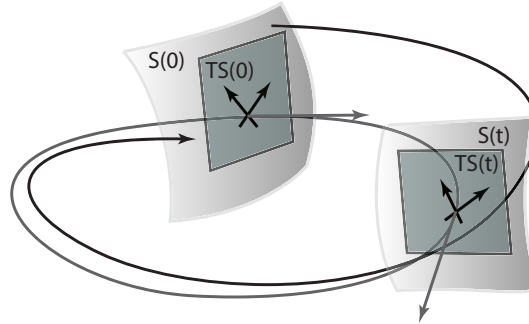


Fig. 2 A visualization of Poincaré surfaces and transverse linearization of a periodic orbit (grey) and a trajectory converging to it (black).

However, the biggest problem for the present study is that the method of Poincaré sections is only defined for periodic orbits. It can be used to study biped walking on flat ground or constant slopes, but on uneven ground where we have no reasonable expectation of periodic orbits it is not applicable.

With this as motivation, in this work we use instead the *transverse linearization* of the target trajectory, which has previously been used for analysis and stabilization of *periodic* motions of nonlinear systems including walking robots [16, 17, 18, 19, 20].

This can be visualized via the related concept of a *moving Poincaré section*, introduced in [21]. This is a continuous family of $(2n - 1)$ -dimensional surfaces transverse to the desired trajectory, with one member of the family present at *every* point along the cycle ($S(t)$ for all t in Fig. 2).

In contrast to the classical Poincaré map, a transverse linearization (or moving Poincaré section) provides a continuous representation of the relationship between controls and transverse coordinates, and can be extended to the study of non-periodic motions.

Stabilizing only the transverse dynamics — as opposed to, e.g., a full-order linear time-varying (LTV) approximation [22] — is particularly useful for underactuated systems, which are often weakly controllable in the direction along the trajectory.

In this paper, we make use of this, and propose a computationally feasible feedback control strategy for the time-varying impulsive linear system that results. Successful experiments demonstrate the feasibility of our approach.

2 Impulsive Mechanical Systems

The mathematical model we consider is that of a nonlinear mechanical system subject to instantaneous impacts. Let q be a vector of generalized coordinates, and u be a vector of forces and torques which can be assigned, then the dynamics of the system can be written like so [23, 24, 14]:

$$\begin{aligned}
M(q)\ddot{q} + C(q, \dot{q})\dot{q} + G(q) &= B(q)u \quad \text{for } q \notin \mathcal{Q} \\
\left. \begin{aligned} q^+ &= \Delta_q q^- \\ \dot{q}^+ &= \Delta_{\dot{q}}(q^-)\dot{q}^- \end{aligned} \right\} & \text{whenever } q^- \in \mathcal{Q},
\end{aligned} \tag{1}$$

where $M(q)$ is the inertia matrix, $C(q, \dot{q})$ is the matrix of Coriolis and centrifugal terms, $G(q)$ is the gradient of the potential energy field, and $B(q)$ describes the effects of actuators on the generalized coordinates. The set \mathcal{Q} represents switching surfaces, e.g. for a walking robot, states at which the foot of the swing-leg hits the ground, and a new step begins.

2.1 Representation of a Planned Motion

Consider an n -degree-of-freedom impulsive mechanical system for which some desired and feasible trajectory has been specified:

$$q(t) = q^*(t) \in \mathbb{R}^n, \quad t \in [0, \infty).$$

Let t_j , $j = 1, 2, \dots$ be the time moments at which an impact occurs, and let $\mathcal{I}_j := [t_j, t_{j+1})$, $j = 1, 2, \dots$ be the time intervals of smooth behaviour in between impulses, and let $\mathcal{I}_0 := [0, t_1)$.

Assumption 1 *There exists $\tau_1 > \tau_2 > 0$ such that $\tau_1 \geq t_{j+1} - t_j \geq \tau_2$ for all j .*

That is, the footsteps do not get infinitely long or infinitely short.

Assumption 2 *For all t_j , the vector $[\dot{q}^*(t)^T \ddot{q}^*(t)^T]^T$ is linearly independent of the $2n - 1$ vectors spanning the tangent plane of the switching surface at $q^*(t)$.*

That is, all impacts are “real” impacts, not grazing touches of the switching surface.

For each interval \mathcal{I}_j , $j = 0, 1, 2, \dots$, choose one generalized coordinate or some scalar function of the generalized coordinates $\theta := \Theta_j(q)$ which evolves monotonically along a desired trajectory.

Remark 1. In the case of the compass-gait walker, which we will consider in Sections 5 and 6 we will take θ to be the “ankle angle”. It is a reasonable assumption that for any useful walking motion, this angle evolves monotonically over any given step. This representation is common in walking robot control [14].

□

Since it evolves monotonically θ can then be considered as a reparametrization of time, and hence the nominal trajectories of all other coordinates over each interval \mathcal{I}_j can be given as well-defined functions of θ :

$$\begin{aligned}
q_1^*(t) &= \phi_1^j(\theta(t)), \\
&\vdots \\
q_n^*(t) &= \phi_n^j(\theta(t)) \quad \forall t \in \mathcal{I}_j.
\end{aligned}$$

Having thus defined the functions $\phi_1^j, \dots, \phi_n^j$, one can define variables representing deviations from the nominal trajectory:

$$\begin{aligned}
y_1(t) &:= q_1(t) - \phi_1^j(\theta(t)), \\
&\vdots \\
y_n(t) &:= q_n(t) - \phi_n^j(\theta(t)) \quad \forall t \in \mathcal{I}_j,
\end{aligned}$$

where $y_m(t) = 0$ for all m implies the system is on the nominal trajectory.

Consider now the quantities θ, y_1, \dots, y_n . These $n + 1$ quantities are excessive coordinates for the system, and hence one can be dropped. Without loss of generality, let us assume we drop y_n , and our new coordinates are $y = [y_1, \dots, y_{n-1}]^T$ and θ .

Remark 2. When the conditions $y_m = 0$ for all m are enforced via feedback action, the functions $\phi_1^j, \dots, \phi_n^j$ are often referred to as *virtual holonomic constraints* [14, 11, 12]. Our control strategy does not require that these constraint be strictly enforced to guarantee stability, they are simply used as a set of coordinates. However, we retain the terminology “virtual constraints”.

□

3 Construction of the Transverse Linearization

A mechanical system’s dynamics along a target motion can be decomposed into two components: a scalar variable θ representing the position *along* the target motion, and a vector x_\perp of dimension $2n - 1$ representing the dynamics *transverse* to the target motion.

A transverse linearization is a time-varying linear system representing of the dynamics of x_\perp close to the target motion. The stabilization of the transverse linearization implies local exponential orbital stabilization of the original nonlinear system to the target motion [16]. The construction of a transverse linearization for an impulsive mechanical system such as a walking robot can be broken down into two parts: the continuous phases and the impacts maps.

3.1 Construction of the Continuous Part of the Transverse Linearization

A method for analytical construction of a transverse linearization for continuous mechanical systems was proposed in [25, 18]. We will use this construction for the continuous phases of the desired walking motion.

The representation of trajectories introduced in the previous section allows us to analytically construct, at any θ , a set of transversal coordinates without solving the nonlinear differential equations of the system. The first $2n - 2$ coordinates are given by the coordinates y given in (2), and their derivatives:

$$\dot{y}_i = \dot{q}_i - \frac{d\phi_i^j(\theta)}{d\theta} \dot{\theta}, \quad i = 1, \dots, n-1$$

defined in each continuous interval \mathcal{I}_j . For a full set of transverse coordinates, one more independent coordinate is required.

For the continuous phase of an underactuated mechanical system, if the relations $y = 0$ are maintained then the dynamics of the coordinate θ take the following form:

$$\alpha(\theta)\ddot{\theta} + \beta(\theta)\dot{\theta}^2 + \gamma(\theta) = 0 \quad (2)$$

where $\alpha(\cdot), \beta(\cdot), \gamma(\cdot)$ are straightforward to compute. An important fact is that a partial closed-form solution of the system (2) can be computed:

$$\dot{\theta}^2 = \psi_p(\theta, \theta_0)\dot{\theta}_0^2 + \Gamma(\theta, \theta_0)$$

where $(\theta_0, \dot{\theta}_0)$ is any point on the desired trajectory of the reduced system (2). That is, $\dot{\theta}^2$ can be computed as a function of θ , analytically.

The variable

$$I = \dot{\theta}^2 - \psi_p(\theta, \theta_0)\dot{\theta}_0^2 - \Gamma(\theta, \theta_0)$$

is then a clear candidate for the final transverse coordinate: it is independent of y and \dot{y} and is zero when the system is on the target motion.

Our complete set of transverse coordinates are then: $x_{\perp} := [I, y^T, \dot{y}^T]^T$.

Now, for systems of underactuation degree one, there exists a partial feedback-linearizing transformation of the form [26]:

$$u = N(y, \theta)^{-1}[v - W(y, \theta, \dot{y}, \dot{\theta})]$$

creating the dynamics $\dot{y} = v$, $\dot{I} = f(\theta, \dot{\theta}, y, \dot{y}, v)$ where f can be calculated analytically.

From this we construct the continuous part of the transverse linearization, with z representing the state of the linearization of the dynamics of x_{\perp} :

$$\dot{z}(t) = A(t)z(t) + B(t)v(t) \quad (3)$$

where $A(t)$ and $B(t)$ are

$$A(t) = \begin{bmatrix} a_{11}(t) & a_{12}(t) & a_{13}(t) \\ 0_{(n-1)} & 0_{(n-1)^2} & I_{(n-1)} \\ 0_{(n-1)} & 0_{(n-1)^2} & 0_{(n-1)^2} \end{bmatrix} B = \begin{bmatrix} b_1(t) \\ 0_{(n-1)^2} \\ I_{(n-1)} \end{bmatrix} \quad (4)$$

where $I_{(n-1)}$ is the $(n-1)$ -dimensional identity matrix, $0_{(n-1)}$ is an $(n-1)$ -dimensional column of zeros, and $0_{(n-1)^2}$ is an $(n-1) \times (n-1)$ matrix of zeros. The functions $N(y, \theta), R(y, \theta, \dot{y}, \dot{\theta}), a_{11}(t), a_{12}(t), a_{13}(t)$, and $b_1(t)$ can be computed analytically, see [25, 18].

3.2 Transverse Linearization of Impacts

Certain care is required in linearizing the impact map. The transversal surfaces are orthogonal in phase space to the target motion, but the switching surfaces will not be in general. Therefore, we must also introduce two projection operators.

Suppose $d\Delta_j$ is the linearization of the impact map at time t_j about the nominal trajectory, then

$$z(t^+) = F_j z(t) \text{ for } t = t_j, j = 1, 2, \dots \quad (5)$$

where $F_j = P_j^+ d\Delta_j P_j^-$

The construction of P_j^+ and P_j^- is given in [20].

The complete hybrid transverse linearization system is given by (3), (4), and (5).

Assumption 3 *The hybrid transverse linearization system is uniformly completely controllable.*

This assumption essentially states that there is sufficient dynamical coupling between the unactuated and actuated links of the system. It is always satisfied with reasonable walking robot designs.

4 Receding-Horizon Control Design

Exponential stabilization of time-varying systems, even linear systems, is a non-trivial problem. For time-invariant or periodic linear systems one can compute constant or periodic gain matrices, respectively, which exponentially stabilize the system. This is not true in general for time-varying systems. A common technique which is computationally feasible is receding-horizon control, also known as model predictive control (see, e.g., [27, 22] and many others). In this section we describe a slightly modified version of receding-horizon control suitable for impulsive linear systems.

The basic strategy is to repeatedly solve a constrained-final-time linear quadratic optimal control problem for the system (3), (4), (5). That is, minimize the following cost function:

$$J(x, u) = \int_{t_i}^{t_f} [z(t)^T Q(t) z(t) + v(t)^T R(t) v(t)] dt + \sum_{j=1}^{N_j} z(t_j)^T Q_j z(t_j)$$

subject to the constraint $z(t_f) = 0$.

Assumption 4 *There exists $\alpha_i > 0$, $i = 0, \dots, 4$, such that $\alpha_0 I \leq Q(t) \leq \alpha_1 I$, $\alpha_2 I \leq R(t) \leq \alpha_3 I$, and $0 \leq Q_j \leq \alpha_4 I$ for all t and j .*

The traditional approach is to set a constant time horizon, but in this work we choose to look a fixed *number of footsteps* ahead¹. Thus, every time the robot takes a footstep, a new optimization is computed.

We propose the following receding-horizon strategy, looking h footsteps ahead, beginning with $i = 0$:

1. Consider the union of intervals $\mathcal{I}_{i,h} := \mathcal{I}_i \cup \mathcal{I}_{i+1} \cup \dots \cup \mathcal{I}_{i+h}$. Let t_i and t_f denote the beginning and end times of $\mathcal{I}_{i,h}$.
2. Compute this footstep's optimal control by solving following jump-Riccati equation backwards in time from t_f to t_i with a final condition $Z(t_f) = 0_{(n-1)^2}$

$$\begin{aligned} -\dot{Z} &= -ZA^T - AZ + BR^{-1}B^T - ZQZ \\ Z(t_j) &= \left\{ F_j^T Z(t_j^+)^{-1} F_j + Q_j \right\}^{-1} \text{ for } t \in \mathcal{I}_j \end{aligned} \quad (6)$$

3. Over the interval \mathcal{I}_i , apply the following state-feedback controller:

$$\begin{aligned} u(y, \theta, \dot{y}, \dot{\theta}) &= N(y, \theta)^{-1} [K(\theta) x_{\perp}(y, \theta, \dot{y}, \dot{\theta}) - W(y, \theta, \dot{y}, \dot{\theta})], \\ K(\theta) &= -R^{-1}(s) B(s)^T Z(s)^{-1}, s = \Theta^{-1}(\theta) \end{aligned} \quad (7)$$

where $\Theta^{-1} : [\theta_+, \theta_-] \rightarrow [t_i, t_{i+1})$ is a projection operator, which is straightforward to construct since θ is monotonic over each step.

4. for the next footstep, set $i = i + 1$ and return to stage 1.

Theorem 1. *If Assumptions 1, 2, 3, and 4 are satisfied, then the controller (6), (7) locally exponentially orbitally stabilizes the planned motion of the original nonlinear system.*

The proof is given in Appendix A.

¹ Or, more generally, a fixed number of impulses ahead.

5 Experimental Setup

We have constructed a two-degree-of-freedom planar biped robot with point feet, a photograph and schematic of which are shown in Fig. 3. The robot is mounted on a boom arm with a counterweight, and thus walks in a circular path. The dynamical effect of the boom is approximated by having different values of hip mass for inertial (m_H) and gravitational (m_{Hg}) terms in the model. The robot is fitted with retractable feet to avoid toe-scuffing, however we do not consider the feet as additional degrees of freedom since their masses are negligible.

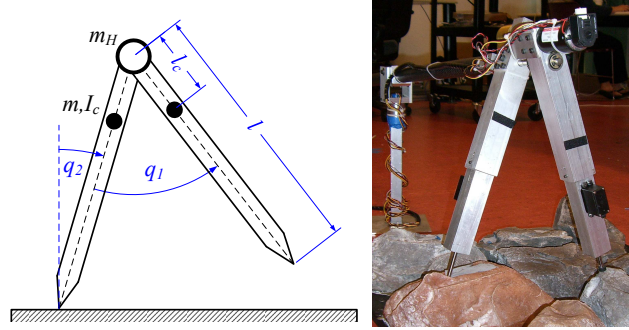


Fig. 3 Schematic and photograph of the experimental setup

The robot is modelled in the form of an impulsive mechanical system (1), the parameters of which were estimated via nonlinear system identification. The full equations for the model are given in Appendix B. Good fitting required the addition of a friction model for the hip joint consisting of Coulomb and viscous parts:

$$\tau_F = F_C \text{sign}(\dot{q}_1) + F_V \dot{q}_1.$$

The parameters of the model are given in Table 1.

The robot is fitted with optical encoders measuring the angle between the legs and the absolute angle of the inner leg. From these measurements q_1 and q_2 can be calculated. The control law relies on velocities as well, and these are estimated with an observer. The observer structure we choose is one which has previously been used successfully in walking robot control, consisting of a copy of the nonlinear dynamics and a linear correction term [28]. Let \hat{q} and $\hat{\dot{q}}$ be the estimates of the configuration states and velocities, then the observer is given by:

$$\begin{aligned} \frac{d}{dt} \begin{bmatrix} \hat{q} \\ \hat{\dot{q}} \end{bmatrix} &= \begin{bmatrix} M(\hat{q})^{-1}(-C(\hat{q}, \hat{\dot{q}})\hat{\dot{q}} - G(\hat{q}) + B(\hat{q})u) \\ \hat{\dot{q}} \end{bmatrix} + L(y - \hat{q}), \\ \hat{q}^+ &= \Delta_q \hat{q}, \quad \hat{\dot{q}}^+ = \Delta_{\dot{q}}(\hat{q})\hat{\dot{q}}, \end{aligned}$$

where y is the measurement of q . The gain L can be chosen as $L = [1/\varepsilon \ 2/\varepsilon^2]$ placing the eigenvalues of the linearized error system at $-1/\varepsilon$. In our experiments we found that $\varepsilon = 0.02$ gave a reasonable compromise between speed of convergence and noise rejection.

Table 1 Parameters of the compass-gait biped.

Parameters	Values
Masses [kg]	$m = 1.3, m_H = 2.2, m_{Hg} = -1.2$
Inertia [kg m ²]	$I_c = 0.0168$
Lengths [m]	$l = 0.32, l_c = l - 0.0596$
Gravitational constant [m/s ²]	$g = 9.81$
Ratio current/input [A]	$k_I = 1.1$
Motor torque constant [Nm/A]	$k_\tau = 0.0671$
Coulomb friction [Nm]	$F_C = 0.02$
Viscous friction [Nm s]	$F_V = 0.01$

5.1 Polynomial Representation of Desired Motion

For the compass biped we take $\theta = q_2$, the “ankle” angle of the stance leg relative to horizontal. Then to specify the path through configuration space for each step j , we need to specify only the inter-leg angle q_1 as a function of the ankle angle: $q_1^* = \phi^j(\theta)$. We chose to construct the ϕ^j functions as fourth-order Bézier polynomials, which can represent a wide range of useful motions with quite a low number of parameters, and furthermore admit simple representations of the constraints in the previous section. For details, see [14, Ch. 6], in which Bézier polynomials were used to design periodic trajectories. It is straightforward to extend this method to non-periodic trajectories and because of space restrictions we omit the details.

6 Experimental Results

To test the controller experimentally, a relatively simple task was chosen: the robot should walk flat for two steps, then down two “stairs”, and then continue along the flat. A video of a successful experiment has been placed online [29].

The control design was implemented as in Section 4 with constant weighting matrices $Q(t) = Q_j = I_3$ and $R(t) = 1$ for all t and j . The look-ahead horizon was chosen as three footsteps ahead.

For each step, the solution of the jump-Riccati equation took approximately half a second to compute using the `ode45` solver in MATLAB running on a Pentium III desktop computer. This is roughly the time it takes for the robot to complete a step, and it is reasonable to expect that highly optimised C code could perform this

task much more quickly. Hence, one can say that the control law could be feasibly computed in real-time, as a part of a dynamic motion-planning and control system.

Figure 4 depicts the results of one experiment. Figure 4(A) is a cartoon of the biped’s motion generated from real data, showing the state every 0.3 seconds, with the current stance leg always indicated in red.

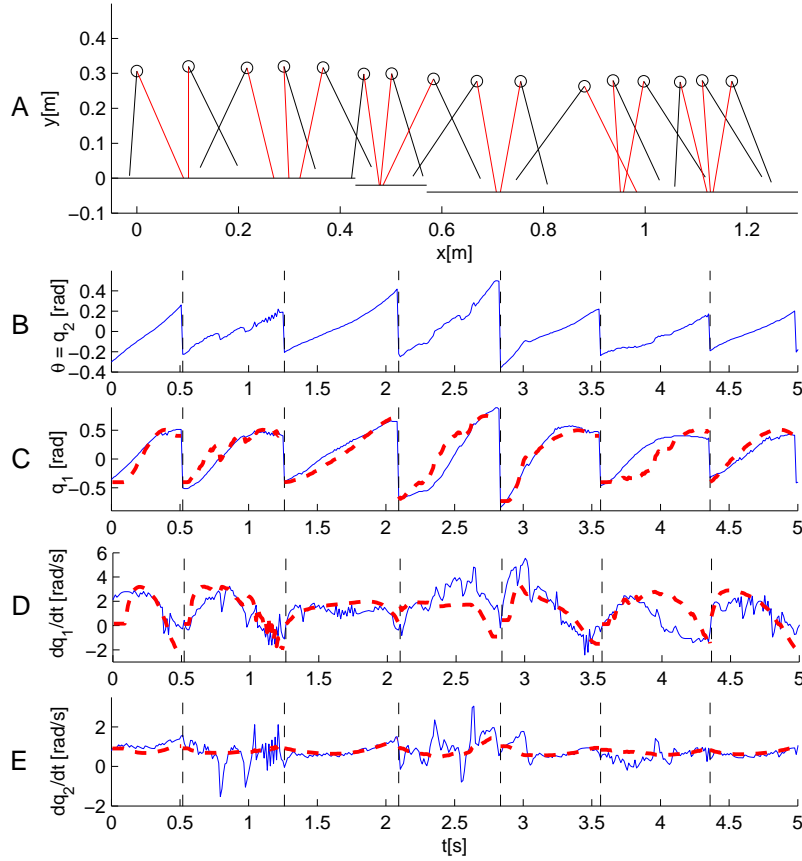


Fig. 4 Results from a successful experiment walking on uneven terrain. See Section 6 for discussion.

In Fig. 4(B) the evolution of the “ankle angle” q_2 is plotted vs time for one experiment. During the continuous phases, q_2 serves as our reparametrization of time θ . We note here that, particularly on the second and fourth steps, there is some jitter in the curve.

In Fig. 4(C) the inter-leg angle q_1 is plotted vs time in blue, along with the “nominal” value of q_1 plotted in red. Note that, since the nominal value of q_1 is not a

function of time but a function of q_2 , defined by the virtual constraint, the jitters in the q_2 measurement lead to jitters in the nominal value of q_1 . Nevertheless, tracking is quite good, and sufficient for the robot to maintain a stable walking trajectory.

Figures 4(D) and (E) depict the joint velocities \dot{q}_1 and \dot{q}_2 , obtained from the same observer used in the control system, along with their nominal values as functions of the current value of q_2 . Again, the jitter in q_2 leads to large noise in the velocity estimates. Despite this, good tracking is maintained through all the planned steps. Repeated experiments were performed with similar results each time, indicating good robustness of the control strategy.

7 Conclusions

In this paper we have described a novel method for stabilization of trajectories of impulsive mechanical systems. The method guarantees local exponential stability to a target orbit under reasonable assumptions. The method is quite general, but a clear target application is motions of underactuated walking robots on rough and uneven terrain. To the authors' knowledge, this is the first systematic control method which can provably stabilize such motions.

The proposed technique was experimentally verified using a compass-gait biped walker. It was seen that, despite measurement errors and inevitable uncertainties in modelling, the controller reliably stabilized the target motions. The method of transverse linearization can be applied to any "dynamic walking" robot to design stabilizing controllers, or to give certificates of stability and assist choice of gains for existing control laws.

Future work will include application to robots with more degrees of freedom on more challenging terrain, and computation of basins of attraction. Furthermore, the theoretical tools developed in this work also have application to problems of motion planning, which will be explored.

8 Appendix A: Proof of Local Stability

Some details are omitted to save space. We consider the Lyapunov function candidate

$$\mathcal{V}(x(t), t, \mathcal{K}) = x(t)^T P(t)x(t)$$

where $P(t) = X(t)^{-1}$, the solution of the finite-time jump-Riccati equation. i.e. the total "cost-to-go" from a state $x(t)$ with a feedback strategy \mathcal{K} defining $u(t) = -K(t)x(t)$

We state the following three facts about this Lyapunov function candidate:

1. It follows from Assumptions 1, 3, and 4 and standard arguments from optimal control [30] that there exists $\beta_1 > \beta_0 > 0$ such that

$$\beta_0 I \leq P(t) \leq \beta_1 I. \quad (8)$$

2. Throughout the continuous phase from t_i to t_{i+1} ,

$$\frac{d}{dt} \mathcal{V}(x(t), t, \mathcal{K}_i) = -x(t)^T [Q(t) + K(t)^T B(t)^T R(t) B(t) K(t)] x(t) < 0.$$

Therefore, it follows from the bounds on $Q(t)$ in Assumption 4 that

$$\frac{d}{dt} \mathcal{V}(x(t), t, \mathcal{K}_i) \leq \alpha_0 \|x(t)\| \quad (9)$$

for all t .

3. Let \mathcal{K}_i refer to the strategy of using finite-time controller calculated at the beginning of step i . Under this strategy, $x(t_{i+h}) = 0$ and remains zero for all $t > t_{i+h}$. After step i , the state is $x(t_{i+1})$. A feasible strategy from here would be to continue with control strategy \mathcal{K}_i . However, a new optimization is performed at step $i+1$ over a new horizon $i+1+h$. Since continuing with \mathcal{K}_i is a feasible strategy, the new optimal strategy \mathcal{K}_{i+1} must have a cost to go

$$\mathcal{V}(x(t_{i+1}), t_{i+1}, \mathcal{K}_{i+1}) \leq \mathcal{V}(x(t_{i+1}), t_{i+1}, \mathcal{K}_i). \quad (10)$$

i.e. the Lyapunov function is non-increasing when an impulse occurs.

From the facts (8), (9), and (10) it follows that the time-varying impulsive linear comparison system (3), (4), (5) is exponentially stable, using a generalization of Lyapunov's second method [31, Ch. 13].

Using Assumptions 1, 2, and 3 arguments similar to those of [25, 18, 20] prove that exponential stability of the transverse linearization implies local orbital exponential stability of the original nonlinear system to the target trajectory.

9 Appendix B: Compass Biped Model

The model of the experimental setup is given by (1) where

$$\begin{aligned} M(q) &= \begin{bmatrix} p_1 & -p_1 + \cos(q_1)p_2 \\ -p_1 + \cos(q_1)p_2 & p_3 + 2p_1 - 2\cos(q_1)p_2 \end{bmatrix}, \\ C(q, \dot{q}) &= \begin{bmatrix} 0 & -\dot{q}_2 \sin(q_1)p_2 \\ -\sin(q_1)(\dot{q}_1 - \dot{q}_2)p_2 & \sin(q_1)\dot{q}_1 p_2 \end{bmatrix}, \quad B = \begin{bmatrix} k_I k_\tau \\ 0 \end{bmatrix}, \\ G(q) &= [\sin(-q_2 + q_1)p_4, -\sin(-q_2 + q_1)p_4 - \sin(q_2)p_5 - \sin(q_2)p_4]^T. \end{aligned}$$

The coefficients are defined by the physical parameters of the robot like so:

$$\begin{aligned} p_1 &= (l-l_c)^2 m + I_c, & p_2 &= ml(l-l_c), & p_3 &= m_H l^2 + 2ml l_c \\ p_4 &= mg(l-l_c), & p_5 &= g(m_H g l + 2ml_c). \end{aligned}$$

The impact model in (1) is derived under the assumption of having an instantaneous and inelastic collision of the swing leg with the ground and no occurrence of slip or rebound [24]:

$$\Delta_q = \begin{bmatrix} -1 & 0 \\ -1 & 1 \end{bmatrix}, \quad \Delta_{\dot{q}}(q^-) = \Delta_q [H^+(q^-)]^{-1} H^-(q^-),$$

where

$$\begin{aligned} H_{1,1}^+(q^-) &= p_1 - 2p_6 l + l^2 p_7, \\ H_{1,2}^+(q^-) &= H_{2,1}^+(q^-) = (l^2 p_7 + (-p_8 - 2p_6)l + p_2) \cos(q_1) - l^2 p_7 + 2p_6 l - p_1, \\ H_{2,2}^+(q^-) &= (-2l^2 p_7 + (2p_8 + 4p_6)l - 2p_2) \cos(q_1) + 2l^2 p_7 + (-4p_6 - 2p_8)l + p_3 \\ &\quad + 2p_1, \\ H_{1,1}^-(q^-) &= p_1 - p_6 l, & H_{1,2}^-(q^-) &= ((-p_6 - p_8)l + p_2) \cos(q_1) - p_1 + p_6 l, \\ H_{2,1}^-(q^-) &= (p_2 - p_6 l) \cos(q_1) - p_1 + p_6 l, \\ H_{2,2}^-(q^-) &= ((2p_6 + p_8)l - 2p_2) \cos(q_1) + (-p_8 - 2p_6)l + p_3 + 2p_1 \\ p_6 &= m(l-l_c) & p_7 &= m_H + 2m, & p_8 &= l_c p_7 + m_H(l-l_c). \end{aligned}$$

References

1. M. Vukobratovic and B. Borovac, "Zero-moment point – thirty five years of its life," *International Journal of Humanoid Robotics*, vol. 1, no. 1, pp. 157–173, 2004.
2. T. McGeer, "Passive dynamic walking," *International Journal of Robotics Research*, vol. 9, no. 2, pp. 62–82, 1990.
3. S. Collins, A. Ruina, R. Tedrake, and M. Wisse, "Efficient bipedal robots based on passive-dynamic walkers," *Science*, vol. 307, no. 5712, pp. 1082–1085, 2005.
4. K. Byl and R. Tedrake, "Approximate optimal control of the compass gait on rough terrain," in *Proc. of the IEEE International Conference on Robotics and Automation*, Pasadena, CA, 2008.
5. F. Iida and R. Tedrake, "Minimalistic control of a compass gait robot in rough terrain," in *Proc. of the IEEE International Conference on Robotics and Automation*, Kobe, Japan, 2009.
6. K. Byl, A. Shkolnik, N. Roy, and R. Tedrake, "Reliable dynamic motions for a stiff quadruped," in *Proc. of the 11th International Symposium on Experimental Robotics (ISER)*, Athens, Greece, 2008.
7. A. Goswami, B. Espiau, and A. Keramane, "Limit cycles in a passive compass gait biped and passivity-mimicking control laws," *Autonomous Robots*, vol. 4, no. 3, pp. 273–286, 1997.
8. F. Asano, M. Yamakita, N. Kamamichi, and Z. W. Luo, "A novel gait generation for biped walking robots based on mechanical energy constraint," *IEEE Transactions on Robotics and Automation*, vol. 20, no. 3, pp. 565–573, 2004.
9. M. Spong, J. Holm, and D. Lee, "Passivity-based control of bipedal locomotion," *IEEE Robotics and Automation Magazine*, vol. 14, no. 2, pp. 30–40, 2007.
10. Y. Hurmuzlu and G. Moskowitz, "The role of impact in the stability of bipedal locomotion," *Dynamics and Stability of Systems*, vol. 1, pp. 217–234, 1986.

11. J. Grizzle, G. Abba, and F. Plestan, "Asymptotically stable walking for biped robots: Analysis via systems with impulse effects," *IEEE Transactions on Automatic Control*, vol. 46, no. 1, pp. 51–64, 2001.
12. E. Westervelt, J. Grizzle, and D. Koditschek, "Hybrid zero dynamics of planar biped walkers," *IEEE Transactions on Automatic Control*, vol. 48, no. 1, pp. 42–56, 2003.
13. M. Wisse, A. Schwab, R. van der Linde, and F. van der Helm, "How to keep from falling forward: elementary swing leg action for passive dynamic walkers," *IEEE Transactions on Robotics*, vol. 21, no. 3, pp. 393–401, 2005.
14. E. Westervelt, J. Grizzle, C. Chevallereau, J. Choi, and B. Morris, *Feedback Control of Dynamic Bipedal Robot Locomotion*. Boca Raton, FL: CRC Press, 2007.
15. D. Hobbelen and M. Wisse, "A disturbance rejection measure for limit cycle walkers: The gait sensitivity norm," *IEEE Transactions on Robotics*, vol. 23, no. 6, pp. 1213–1224, 2007.
16. J. Hauser and C. Chung, "Converse Lyapunov function for exponential stable periodic orbits," *Systems and Control Letters*, vol. 23, pp. 27–34, 1994.
17. A. Banaszuk and J. Hauser, "Feedback linearization of transverse dynamics for periodic orbits," *Systems and Control Letters*, vol. 26, pp. 95–105, 1995.
18. A. S. Shiriaev, L. B. Freidovich, and I. R. Manchester, "Can we make a robot ballerina perform a pirouette? Orbital stabilization of periodic motions of underactuated mechanical systems," *Annual Reviews in Control*, vol. 32, no. 2, pp. 200–211, 2008.
19. L. B. Freidovich, A. S. Shiriaev, and I. R. Manchester, "Stability analysis and control design for an underactuated walking robot via computation of a transverse linearization," in *Proceedings of the 17th IFAC World Congress*, Seoul, Korea, Jul. 6-11 2008.
20. A. S. Shiriaev, L. B. Freidovich, and I. R. Manchester, "Periodic motion planning and analytical computation of transverse linearizations for hybrid mechanical systems," in *Proceedings of the 47th IEEE Conference on Decision and Control*, Cancun, Mexico, 2008.
21. G. Leonov, "Generalization of the Andronov-Vitt theorem," *Regular and chaotic dynamics*, vol. 11, no. 2, pp. 281–289, 2006.
22. D. Q. Mayne, J. B. Rawlings, C. V. Rao, and P. O. M. Scokaert, "Constrained model predictive control: Stability and optimality," *Automatica*, vol. 36, no. 6, pp. 789–814, 2000.
23. M. Spong, S. Hutchinson, and M. Vidyasagar, *Robot Modeling and Control*. New Jersey: John Wiley and Sons, 2006.
24. Y. Hurmuzlu and D. Marghitu, "Rigid body collisions of planar kinematic chains with multiple contact points," *The International Journal of Robotics Research*, vol. 13, no. 1, pp. 82–92, 1994.
25. A. Shiriaev, J. Perram, and C. Canudas-de-Wit, "Constructive tool for orbital stabilization of underactuated nonlinear systems: virtual constraints approach," *IEEE Transactions on Automatic Control*, vol. 50, no. 8, pp. 1164–1176, 2005.
26. M. Spong, "Partial feedback linearization of underactuated mechanical systems," in *Proc. of International Conference on Intelligent Robots and Systems*, Munich, Germany, 2004.
27. W. Kwon, A. Bruckstein, and T. Kailath, "Stabilizing state-feedback design via the moving horizon method," *International Journal of Control*, vol. 37, no. 3, pp. 631–643, 1983.
28. J. Grizzle, J. Choi, H. Hammouri, and B. Morris, "On observer-based feedback stabilization of periodic orbits in bipedal locomotion," in *Proc. Methods and Models in Automation and Robotics*, 2007.
29. http://groups.csail.mit.edu/locomotion/movies/cgexperiment20081222_4.mov.
30. R. Kalman, "Contributions to the theory of optimal control," *Bol. Soc. Mat. Mexicana*, vol. 5, pp. 102–119, 1960.
31. D. Bainov and P. Simeonov, *Systems with Impulse Effects: Stability, Theory and Applications*, ser. Ellis Horwood Series: Mathematics and its Applications. Chichester: Ellis Horwood, 1989.